

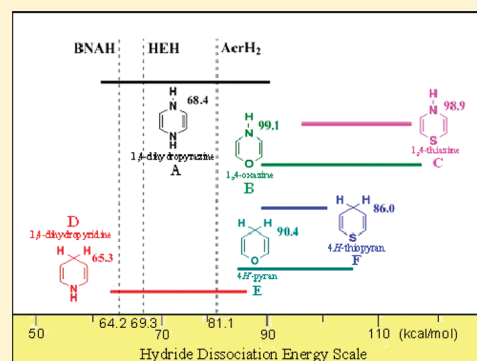
Hydride Dissociation Energies of Six-Membered Heterocyclic Organic Hydrides Predicted by ONIOM-G4Method

Jing Shi,* Xiong-Yi Huang, Hua-Jing Wang, and Yao Fu

Department of Chemistry, University of Science and Technology of China, Hefei 230026, China

Supporting Information

ABSTRACT: Hydride dissociation energy is of great importance in understanding the hydride-donating abilities of organic hydrides. Although the hydride dissociation energies of some organic hydrides have been experimentally measured, much less attention has been focused on the investigation of these quantities from the first principles of physics. Herein, we developed an ONIOM-G4 method and carefully benchmarked this new method against 48 experimental hydride dissociation energies of diverse bulky molecules. It was found that with the combined methods of the HF/6-31+G(d,p)//IEFPCM/Bondi1.15 solvation model, the ONIOM-G4 method can predict the hydride dissociation energies with an error bar of only 1.7 kcal/mol. With the newly developed ONIOM-G4 method, we then systematically studied the hydride dissociation energies of six categories of biologically and pharmaceutically important six-membered heterocyclic organic hydrides, namely, the organic hydrides containing 1,4-dihydropyridine, 1,4-dihydropyrazine, 1,4-oxazine, 1,4-thiazine, 4H-pyran, and 4H-thiopyran ring structures. An extensive hydride dissociation energy scale containing over 100 six-membered heterocyclic organic hydrides has been established, which may find applications in both synthetic organic chemistry and mechanistic studies of various chemical or biological processes involving transferring of the hydride anion.



1. INTRODUCTION

Natural organic hydride donors like FADH₂,^{1–4} NAD(P)H,^{5–7} ascorbic acid (vitamin C), and tetrahydrofolate are important in many biochemical processes.^{8–10} Man-made organic hydrides, which mimic the structures of natural organic hydrides, have very broad applications. For example, they can be used as models of some natural organic hydrides to study the biological hydride transfer processes,^{11–22} as reducing agents in organic synthesis,^{23–30} as building blocks to construct molecular devices,^{31–36} as basic structures to design new materials for hydrogen storage,^{37,38} and as molecular probes to study living phenomena.^{39–42} Although the mechanisms of the hydride transfer step in many biochemical and chemical reactions have been extensively studied for decades,^{43–50} much less attention has been paid to the thermodynamic properties of organic hydrides.^{51,52} Among various thermodynamic properties, the hydride dissociation energy, which expresses the enthalpy changes of the hydride anion dissociation process, is one of the most important thermodynamic properties of organic hydrides. It is the quantitative measurement of hydride-donating abilities of organic hydrides and can provide important information about the thermodynamic driving force of various processes involving transfer of hydride.

Early studies of hydride dissociation energies exclusively focused on several model compounds mimicking nicotinamide adenine dinucleotide phosphate (NADPH),^{53–58} such as 1-benzyl-1,4-dihydronicotinamide (BNAH), 9,10-dihydroacridine (AcH₂), and Hantzsch esters (HEH). During the past 10 years, the scale has

been considerably expanded, mainly due to the systematic studies of Cheng and Zhu. In their work, detailed thermodynamic analysis has been conducted on various types of organic hydrides and hydride acceptors, including hydrides with basic structures of 1,4-dihydro-pyridine,^{39,53,59} 2,3-dihydroimidazole, 2,3-dihydrothiazole, 2,3-dihydrooxazole,⁶⁰ and hydride acceptors like olefins,⁶¹ dienes,⁶² phenothiazines,⁶³ and imines.⁶⁴ However, the hydride-donating abilities of several types of biologically and pharmaceutically important organic hydrides, especially six-membered heterocyclic organic hydrides with basic structures of 4H-pyran, 4H-thiopyran, 1,4-oxazine, and 1,4-dihydropyrazine, are still less investigated. These six-membered heterocyclic compounds are prevalent in biological and pharmaceutical systems; i.e., the 1,4-dihydropyrazine ring is the active center of FADH₂, FMNH₂, and tetrahydrofolic acid;^{1–4} the 1,4-oxazine ring is the key structure of actinomycin antibiotics;^{65,66} and the pyrylium cation (the product of 4H-pyran after hydride dissociation) is ubiquitous in plant pigments such as anthocyanin.^{67–70} Therefore, it is desirable to systematically study the hydride dissociation energies of these six-membered heterocyclic organic hydrides.

However, due to the sophistication and laboriousness of the current experimental method to measure the hydride dissociation energies, the systematic study of all of these categories of six-membered heterocyclic organic hydrides through experimentation would be a difficult task. Recent development of

Received: April 6, 2011

Published: December 7, 2011

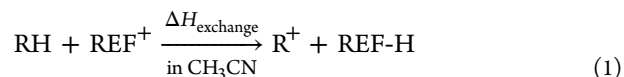
computational chemistry provides us an alternative way to study the hydride dissociation energy. The B3LYP^{71,72} density functional has been used for calculating the hydride affinity of quinones, with a maximum error of 5 kcal/mol.⁷³ Some of the latest studies have shown that popular density functionals (e.g., B3LYP) can systematically underestimate reaction energies in treatments of organic compounds.^{74–77} In order to accurately calculate molecular energies, a variety of composite quantum chemistry procedures have been developed, including Gaussian (Gn) models,^{78–82} Weizmann (Wn) methods,^{83–85} and complete-basis-set (CBS) procedures.^{86–88} The newly developed G4 theory has been shown to achieve an average absolute deviation of 0.83 kcal/mol for a test set of 454 energies.⁸¹ The emergence of this new high level method intrigues us and moves us to examine its ability to calculate the hydride dissociation energy. However, similar to the other high level methods, G4 is restricted to small molecules due to its high computational cost.^{89–92} Our previous studies have shown that the combination of the ONIOM approach and G3 theory can expand the G3-type method to sizable molecules with high accuracy in energy calculation.^{93–95} Therefore, we decide to develop the ONIOM-G4 method and test its performance in estimating hydride dissociation energy.

We aim to accomplish two tasks in this study: (1) to develop a theoretical protocol at the G4 level of theory to accurately calculate the hydride dissociation energies and (2) to systematically study the hydride dissociation energies of various types of six-membered heterocyclic organic hydrides. This study would be beneficial for understanding hydride donating and accepting abilities of various organic compounds and provide further insight into the related hydride transfer reactions.

2. METHOD DEVELOPMENT

2.1. General Method for the Calculation of the Hydride Dissociation Energies. The reaction $\text{RH} \rightarrow \text{R}^+ + \text{H}^-$ is the direct formulation to calculate the hydride dissociation energy of the organic hydride, RH. However, there will be large computational error when using this formulation, mainly due to two aspects. First, the computational error of the solvation free energies of the hydride anion is large. Second, considering that there are two ionic species at one side of the reaction and a neutral species at the other side, the computational error in solvation free energies is further exacerbated. These drawbacks can be overcome by choosing the following hydride exchange

reaction (eq 1).



REF refers to the reference molecule, whose hydride dissociation energy is accurately experimentally measured. If the experimental hydride dissociation energy of the reference molecule is designated as $\Delta H_{\text{H}^-}(\text{REF})$, the hydride dissociation energy of RH can be readily calculated using eq 2. The gas-phase part can be handled by standard quantum chemical methods, whereas the solvation free energies are calculated by the polarized continuum (PCM) solvation model.^{96–98}

$$\Delta H_{\text{H}^-}(\text{RH}) = \Delta H_{\text{H}^-}(\text{REF}) + \Delta H_{\text{exchange}} \quad (2)$$

We begin our study by evaluating the performance of various theoretical methods against a benchmark set containing 11 typical organic hydrides (Figure 1). In a similar way to that for the experimental measurement,⁹⁹ 9,10-dihydroacridine (AcrH₂) is selected as the reference molecule.

2.2. Computational Methodology. All calculations were done with the Gaussian 03 suite of programs.⁹⁹ The geometries were fully optimized using the hybrid density functional B3LYP in combination with the 6-31G(2df,p)^{100,101} basis set. But for ONIOM-G3B3 calculation, the 6-31G(d)^{100,101} basis set was used for geometry optimization to be consistent with the requirement of a G3B3 level of theory. For the molecules which have more than one possible conformation, the conformation with the lowest Gibbs free energy was singled out and used in the ensuing calculations. Each optimized geometry was confirmed to be a real minimum on the potential energy surface without any imaginary frequency. The harmonic vibrational frequencies, zero point energies (ZPE), and thermal corrections to enthalpy were computed at the optimized geometry using the same level of theory. A scaling factor of 0.9854 for the calculated ZPE was used. For the calculation of single-point energies, a larger basis set, 6-311++G(2df,p),^{102–109} was used in conjugation with a variety of density functionals selected for evaluation. It is worth noting that all calculated gas-phase energies correspond to the reference state of 1 atm and 298 K. For the calculation of solvation energies, the integral equation formalism of the PCM^{110–112} solvation model (IEF-PCM)^{113,114} was used. All of the IEF-PCM calculations were performed at the HF/6-31+G(d, p)^{100,101} level of theory (Icomp = 4, TSNUM = 60, TSARE = 0.4,

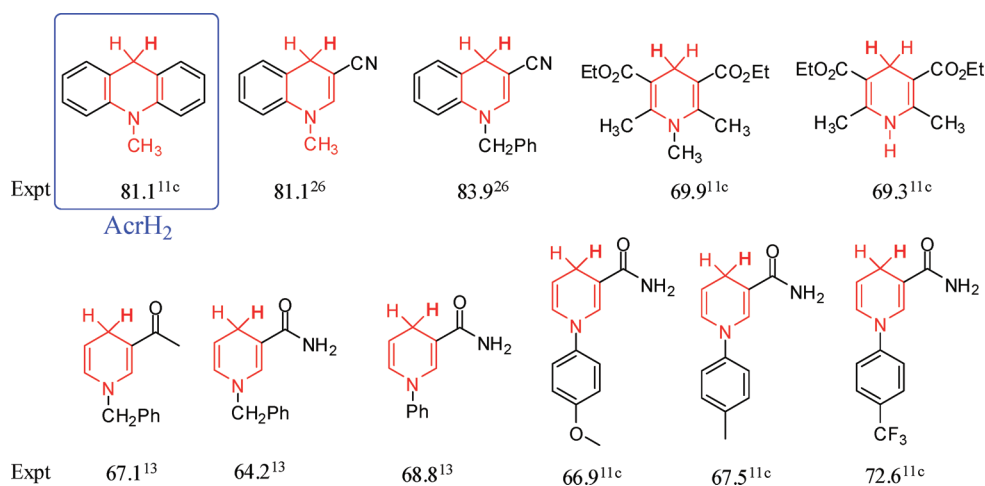


Figure 1. Eleven typical organic hydrides for the evaluation of different methods (the core layer used in the ONIOM approach is highlighted in red).

Table 1. Performance of Different Theoretical Methods for Estimating the Hydride Dissociation Energies of the Benchmark Molecules (unit: kcal/mol)

entry	method	basis set for geometry optimization	basis set for energy calculation	solvation model	rms error	maximum error	R^a	mean error
1	B3LYP	6-31G(2df, p)	6-311++G(2df, p)	HF//IEFPCM/Bondi1.35	3.5	5.8	0.960	2.7
2	MP2	6-31G(2df, p)	6-311++G(d,p)	HF//IEFPCM/Bondi1.35	5.0	7.2	0.954	4.1
3	X3LYP	6-31G(2df, p)	6-311++G(2df, p)	HF//IEFPCM/Bondi1.35	3.4	5.7	0.971	2.6
4	B3P86	6-31G(2df, p)	6-311++G(2df, p)	HF//IEFPCM/Bondi1.35	2.9	5.1	0.968	2.2
5	B3PW91	6-31G(2df, p)	6-311++G(2df, p)	HF//IEFPCM/Bondi1.35	2.9	5.0	0.958	2.3
8	ONIOM-G3B3	6-31G(d)		HF//IEFPCM/Bondi1.35	2.8	5.1	0.969	2.1
9	ONIOM-G3B3	6-31G(d)		HF//IEFPCM/Bondi1.25	2.6	5.1	0.970	2.0
10	ONIOM-G3B3	6-31G(d)		HF//IEFPCM/Bondi1.15	2.5	4.7	0.971	1.7
11	ONIOM-G3B3	6-31G(d)		HF//IEFPCM/Bondi1.05	2.5	5.3	0.970	1.7
12	ONIOM-G3B3	6-31G(d)		HF//IEFPCM/ua0	3.4	5.9	0.941	2.3
13	ONIOM-G3B3	6-31G(d)		HF//IEFPCM/uahf	2.8	10.0	0.881	4.3

^a R is the correlation coefficient between the theoretical and experimental BDEs.

radii = bondi, $\alpha = 1.15$). The geometries optimized in the gas phase were used for the solution-phase calculations, as it has been demonstrated that the change of geometry by the solvation effect is usually not significant for relatively rigid organic molecules.^{115,116} All of the solution-phase energies reported in the paper correspond to the reference state of 1 mol/L, 298 K.

2.3. Evaluation of Different Theoretical Methods.

With the structures optimized at the B3LYP/6-31G(2df,p) level of theory and solvation energies calculated with the HF/6-31+G(d,p)//IEFPCM/Bondi1.35 level of theory, we first evaluated the theoretical methods used for the calculation of single-point energies. Møller–Plesset (MP2)^{117–121} perturbation theory and four density functionals, including B3LYP, X3LYP,¹²² B3PW91,¹²³ and B3P86,¹²⁴ were examined. It is found that all selected methods fail to accurately estimate the hydride dissociation energies of the benchmark molecules (see Table 1). The RMS (root of mean square) errors for the MP2, B3PW91, B3P86, and B3LYP levels of theory are 5.0, 2.9, 2.9, and 3.5 kcal/mol, respectively. The X3LYP density functional, which was developed recently and has been shown to be capable of accurately calculating the thermodynamic properties of organic compounds,¹²⁵ has an RMS error of 4.6 kcal/mol. Besides, we also tested the performance of a high level composite *ab initio* method, ONIOM-G3B3. It gives a better result with an RMS error of 2.8 kcal/mol. On the basis of the ONIOM-G3B3 level of theory, we then evaluate different solvation models. It is found that the use of a scaling factor of 1.15 for the bond radii can further improve the accuracy to an RMS error of 2.5 kcal/mol. However, this error is still larger than the common error bar of the experimental measurement (i.e., 1.0–2.0 kcal/mol).

2.4. Development of the ONIOM-G4 Method and Its Performance in Calculating Hydride Dissociation Energies. The ONIOM approach was developed by Morokuma and co-workers in the 1990s.¹²⁶ It divides a sizable molecule into different layers and applies different levels of theory to different layers as well as the whole molecule. For the two-layered ONIOM approach, only the core layer is treated with the high level of theory. The integrated total energy of a two-layer system was calculated by eq 3.

$$E(\text{ONIOM}) = E(\text{high, core layer}) + E(\text{low, whole system}) - E(\text{low, core layer}) \quad (3)$$

“High” and “low” refer to a high level of theory and a low level of theory that are chosen for the two-layered ONIOM approach. For the ONIOM-G4 level of theory, we choose G4 as the high level of theory and B3LYP/6-31G(2df, p) as the low level of theory. The detailed procedure of ONIOM-G4 theory is shown in Table 2. Therefore, the geometry of the

Table 2. Detailed Procedure of the ONIOM-G4 Theory

geometry	ONIOM-G4
	B3LYP/6-31G(2df, p)
single-point energies ^a	ONIOM(MP4/6-31G(d):B3LYP/6-31G(2df, p)) (A) ONIOM(MP2/6-31G(d):B3LYP/6-31G(2df, p)) (A1) ONIOM(MP4/6-31+G(d):B3LYP/6-31G(2df, p)) (B) ONIOM(MP2/6-31+G(d):B3LYP/6-31G(2df, p)) (B1) ONIOM(MP4/6-31G(2df, p):B3LYP/6-31G(2df, p)) (C) ONIOM(MP2/6-31G(2df,p):B3LYP/6-31G(2df, p)) (C1) ONIOM(CCSd(T)/6-31G(d):B3LYP/6-31G(2df, p)) (D) ONIOM(MP2(full)/G3LargeXP:B3LYP/6-31G(2df,p)) (E) ONIOM(HF/aug-cc-pVQZ:B3LYP/6-31G(2df, p)) (F1) ONIOM(HF/aug-cc-pVSZ:B3LYP/6-31G(2df, p)) (F2) ONIOM(HF/G3LargeXP:B3LYP/6-31G(2df, p)) (F3)
higher-level correction (ΔHLC) ^b	closed shell: $-A n_\beta$ open shell: $-A' n_\beta - B(n_\alpha - n_\beta)$ atoms and atom ions: $-C n_\beta - D(n_\alpha - n_\beta)$ third-row species (K, Ca, and Ga–Kr): $-C n_\beta - D(n_\alpha - n_\beta) - E$ $A = 6.947$ millihartree, $B = 2.441$ millihartree $C = 7.116$ millihartree, $D = 1.414$ millihartree $A' = 7.128$ millihartree, $E = 2.745$ millihartree
Zero-point energy (ZPE) ^c	B3LYP/6-31G(2df, p)

^a $E_0(\text{ONIOM-G4B3}) = E(A) + \Delta E(+) + \Delta E(2df,p) + \Delta E(CC) + \Delta E(G3LargeXP) + \Delta E(HF) + \Delta E(SO) + E(\Delta\text{HLC}) + E(\text{ZPE})$, where $\Delta E(+) = E(B) - E(A)$, $\Delta E(2df,p) = E(C) - E(A)$, $\Delta E(CC) = E(D) - E(A)$, $\Delta E(G3LargeXP) = E(E) - E(C1) - E(B1) + E(A1)$, $\Delta E(HF) = (E(F2) - E(F1) \exp(-1.63))/(1 - \exp(-1.63)) - E(F3)$, $\Delta E(SO)$. ^b n_α and n_β are the number of α and β valence electrons, respectively, with $n_\alpha \geq n_\beta$. A, B, C, D, E, A' are in millihartrees. ^cScale factor of 0.9854 for B3LYP/6-31G(2df, p). ^dFor the present study, the $E(\Delta\text{HLC})$ term is canceled out by using isodesmic eq 1.

whole system is optimized with the B3LYP/6-31G(2df, p) level of theory. Then, following the same procedure of G4 theory, a series of single-point energy calculations is performed by using the two-layered ONIOM approach. The final ONIOM-G4 energy is calculated using an extrapolation equation, as

Table 3. Performance of ONIOM-G4 Theory for the 11 Typical Organic Hydrides (unit: kcal/mol)

entry	method	basis set for geometry optimization	solvation model	RMS error	maximum error	R^a	mean error
1	ONIOM-G4	6-31G(2df, p)	HF//IEFPCM/Bondi1.15	1.8	3.3	0.972	1.5
2	ONIOM-G4	6-31G(2df, p)	HF//IEFPCM/Bondi1.35	2.1	3.7	0.977	1.6
3	ONIOM-G4	6-31G(2df, p)	HF//IEFPCM/Bondi1.25	2.0	3.6	0.975	1.5
4	ONIOM-G4	6-31G(2df, p)	HF//IEFPCM/Bondi1.05	2.0	3.3	0.967	1.6
5	ONIOM-G4	6-31G(2df, p)	HF//IEFPCM/Bondi1.0	3.0	6.4	0.906	2.2
6	ONIOM-G4	6-31G(2df, p)	HF//IEFPCM/ua0	2.7	5.7	0.920	2.1
7	ONIOM-G4	6-31G(2df, p)	HF//IEFPCM/uahf	4.1	8.1	0.886	2.9

^a R is the correlation coefficient between the theoretical and experimental BDEs.

shown in Table 2. This equation is directly derived from the extrapolation equation using the G4 theory. Then, to calculate the thermodynamic properties of the molecule, we next convert the ONIOM-G4 energies to the enthalpy values at 298 K and 1 atm, by adding the standard temperature correction terms H_{trans} , H_{rot} , and H_{vib} . These terms are calculated at the B3LYP/6-31G(2df, p) level of theory using the equilibrium statistical mechanics with harmonic oscillator and rigid rotor approximations. The strategy to partition the system into a high-level region and a low-level region in ONIOM-G4 theory is the same as that used in the ONIOM-G3B3 theory.⁹³

We then calculate the hydride dissociation energies of the 11 selected organic hydrides using the newly developed ONIOM-G4 theory. The results are shown in Table 3. It is found that with the application of the HF//IEFPCM/Bondi1.15 solvation model and ONIOM-G4 theory, the accuracy of estimating hydride dissociation energies can be increased to 1.8 kcal/mol (entry 1, Table 3). A further optimization of solvation models reveals that HF//IEFPCM/Bondi1.15 is the optimal solvation model to be used in combination with the ONIOM-G4 level of theory. To further confirm the reliability of the ONIOM-G4//HF//IEFPCM/Bondi1.15 level of theory to calculate hydride dissociation energies, we next predicted the hydride dissociation energies of another 48 organic hydrides (detailed data are tabulated in the Supporting Information, Table S5). The results are shown in Figure 2. The theoretical predictions are found to

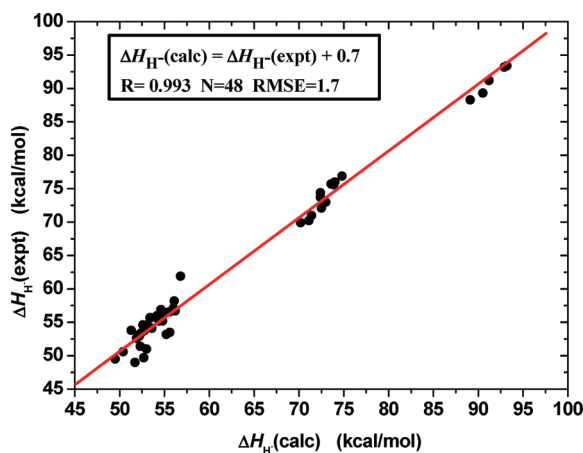


Figure 2. Correlation between the experimental and hydride dissociation energies predicted with the ONIOM-G4//HF//IEFPCM/Bondi1.15 level of theory.

be in good agreement with the experimental data. The correlation coefficient between the theoretical and experimental hydride dissociation energies is 0.993 (see Figure 2). The RMS error is 1.7 kcal/mol, which is comparable to the error bar of the experimental measurement (i.e., 1–2 kcal/mol).

3. RESULTS AND DISCUSSION

3.1. Extensive Scale of Six-Membered Heterocyclic Organic Hydrides. With the validated theoretical method developed above, we calculated the hydride dissociation energies of 104 six-membered heterocyclic hydrides. According to their basic ring structures, these 104 organic hydrides can be divided into six categories, that is, 1,4-dihydropyrazine (A), 1,4-oxazine (B), 1,4-thiazine (C), 1,4-dihydropyridine (D), 4H-pyran (E), and 4H-thiopyran (F). All six of these categories of organic hydrides are important in biological and pharmaceutical systems.^{8–10,65–70} The hydride dissociation energy scales of different categories are summarized in Figure 3.

As shown in Figure 3, hydride dissociation energies of organic hydrides with basic ring structures of 1,4-oxazine, 1,4-thiazine, 4H-pyran, and 4H-thiopyran are all larger than that of AcH_2 , a well-known weak organic hydride donor, suggesting that they are weak hydride donors. But for organic hydrides with basic ring structures of 1,4-dihydropyridine and 1,4-dihydropyrazine, the hydride dissociation energies cover all three regions, indicating that the hydride donating abilities of these two categories can be readily tuned. The hydride dissociation energies of these six categories of organic hydrides generally increase in the following order: 1,4-dihydropyridine (65.3 kcal/mol) < 1,4-dihydropyrazine (68.4 kcal/mol) < 4H-thiopyran (86.0 kcal/mol) < 4H-pyran (90.4 kcal/mol) < 1,4-thiazine (98.9 kcal/mol) \approx 1,4-oxazine (99.1 kcal/mol).

Several interesting points can be raised by close scrutiny of the energy scales shown in Figure 3. First, organic hydrides with ring structures of 1,4-dihydropyridine and 1,4-dihydropyrazine are much stronger hydride donors than the other four categories. The corresponding hydride dissociation energies of 1,4-dihydropyridine and 1,4-dihydropyrazine are more than 20 kcal/mol lower than those of 4H-thiopyran, 4H-pyran, 1,4-thiazine, and 1,4-oxazine. This might partly explain why NAD(P)H, NADH (both with ring structures of 1,4-dihydropyridine), and FMNH₂ (with ring structure of 1,4-dihydropyrazine) are chosen by nature as the hydride source in biological systems. Second, organic hydrides with ring structures of 1,4-dihydropyridine and 1,4-dihydropyrazine have comparable hydride dissociation energies, indicating that the hydride transfer between these two categories would be reversible. This is consistent with the fact that both FMNH₂:NAD(P)⁺ oxidoreductase and NAD(P)H dehydrogenase (FMN) are known in the biological systems ($\Delta\Delta H_{\text{H}}$ between NAD(P)H and FMNH₂ is only 0.2 kcal/mol, see Table 4).^{127–129} Third, organic hydrides with a C–H hydride center are better hydride donors than their N–H counterparts, presumably because the less electron negative carbon atom will better accommodate the positive charges formed during the process of hydride dissociation.

3.2. Substituent Effects on Various Six-Membered Heterocyclic Hydrides. In this section, we calculate the

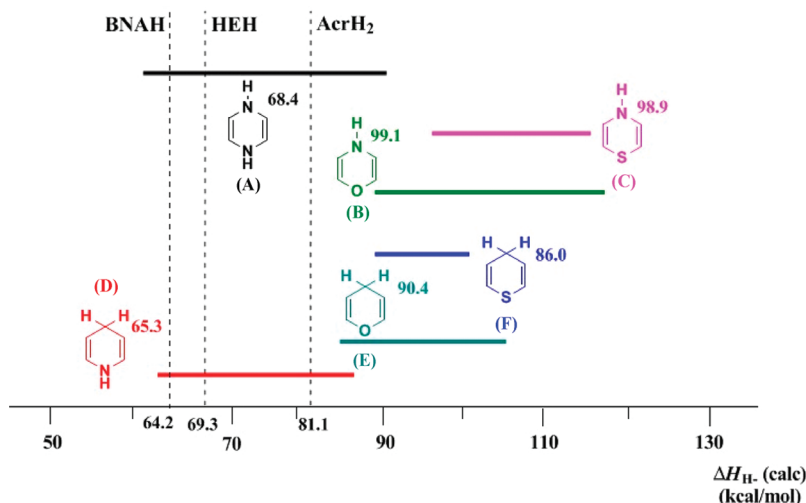
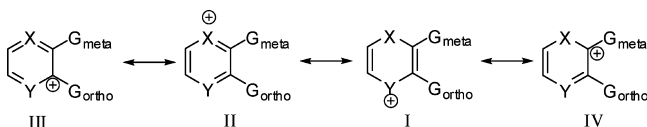


Figure 3. Hydride dissociation energy scales of different categories of six-membered heterocyclic hydrides.

hydride dissociation energies of organic hydrides with various substituents at *ortho* and *meta* positions relative to the hydride center. On the basis of the calculated hydride dissociation energy data, a classic Hammett type correlation analysis is conducted between the ΔH_{H^-} and the substituent constant, σ_p .¹³⁰ The results are summarized in Table 5. The structures of the selected six-membered heterocyclic hydrides are shown in Figure 4.

It can be seen from Table 5 that all six categories of heterocyclic hydrides have good correlation coefficients (from 0.912 to 0.984) and large positive slopes (from 13.0 to 24.9). This indicates that the electron-withdrawing group (EWG) will increase the hydride dissociation energy and decrease the hydride-donating ability of the six-membered heterocyclic hydrides, whereas the electron-donating group (EDG) will decrease the dissociation energy and increase the hydride-donating ability of the six-membered heterocyclic hydrides.

It would be interesting to make a comparison between the *ortho* and *meta* substituent effects. Previous research suggests that such a comparison can be used to understand the distributions of positive charge on the heterocyclic ring.⁶³ After hydride dissociation, the positive charge can be either mainly distributed on heteroatom X (structure II) or on hydride center Y (structure I). The argument is that if the positive charge is mainly distributed on the hydride center Y, then the *meta* substituent Z will exert a stronger effect on the positive charge center through resonance structure IV, leading to a stronger *meta* substituent effect. Accordingly, if X is the positive charge center, then the *ortho* substituent effect will be stronger.



For the six categories of organic hydrides studied here, it is found that the *meta* substituent effect is always stronger than the *ortho* substituent effect. As shown in Table 5, the slopes of the correlation equation of 2A, 2B, 2C, 2D, 2E, and 2F are all larger than those of 1A, 1B, 1C, 1D, 1E, and 1F. This seems to suggest that, for six-membered heterocyclic hydrides, after hydride dissociation, the positive charge will be mainly distributed on the hydride center, Y. To further examine this point, a natural population analysis (NPA)¹³² has been performed (see Figure 5).

From Figure 5, it is found that, for categories A (1,4-dihydropyrazine), B (1,4-oxazine), D (1,4-dihydropyridine), and E (4H-pyran), the positive charge is not mainly distributed on the hydride center, although they have a larger *meta* substituent effect, instead, for these four categories of organic hydrides, *meta* carbon is the positive charge center after hydride dissociation. The charges (including that on the adjacent hydrogen) on *meta* carbon atoms are 0.335, 0.528, 0.335, and 0.543 for categories A, B, D, and E, respectively, while the charges on the hydride centers for these four categories are only -0.315 , -0.217 , 0.174 , and 0.229 . Although smaller than that on the *meta* carbon, the *ortho* carbon atom also shows a large distribution of positive charge (0.303, 0.272, 0.057, and 0.022 for categories A, B, D, and E). These results suggest that the difference between *meta* and *ortho* substituent effects can reflect the relative importance of resonance structures III and IV in stabilizing the positive charges. And the claim that positive charge can be either mainly distributed on the heteroatom or on the hydride center is highly suspect.

However, for categories C (1,4-thiazine) and F (4H-thiopyran), the situation is different from that of the four categories discussed above. In contrast with categories A, B, D and E, for categories C and F, after hydride dissociation, the positive charge is mainly distributed on the *ortho* carbon, although they show a larger *meta* substituent effect. A close scrutiny of the charge distribution reveals that the sulfur atoms in C and F are most likely responsible for this difference. Due to the great ability of the sulfur atom to accommodate positive charges, in C and F, the positive charges are mainly distributed on sulfur (0.776 and 0.712 for categories C and F). In other words, resonance structure II is the only important structure for C and F. Consequently, *meta* and *ortho* substituent effects can only reflect the inductive effect of the substituent on the positive charge center; therefore, it is understandable that they fail to reflect relative charge distributions on the adjacent carbon atom. As the *meta* substituent is closer to the sulfur than the *ortho* substituent, the *meta* substituent would exert a much stronger inductive effect on the positive charge center and lead to a stronger *meta* substituent effect.

3.3. Effect of Aromaticity on Hydride Dissociation Energy. An inspection of the available data reveals that increasing the size of the π system will increase the hydride dissociation energy. As shown in Figure 6, fusing benzene rings

Table 4. Extensive Hydride Dissociation Energy Scales of Six-Membered Heterocyclic Hydrides (unit: kcal/mol, core layer is highlighted in red)

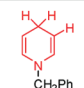
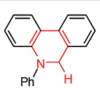
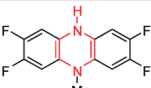
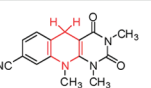
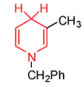
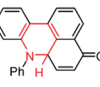
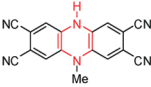
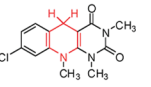
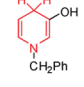
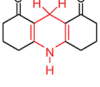
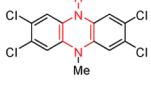
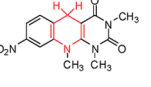
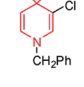
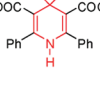
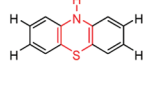
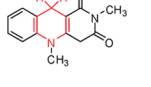
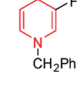
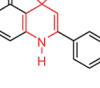
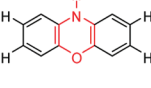
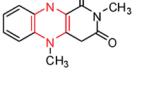
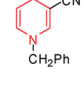
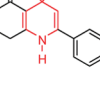
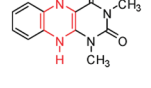
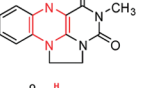
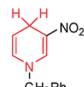
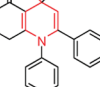
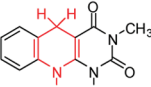
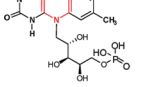
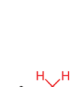
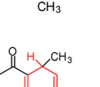
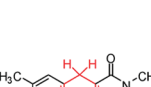
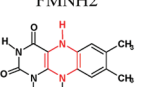
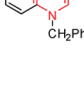
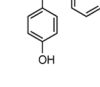
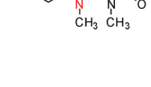
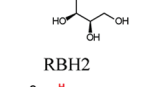
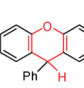
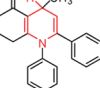
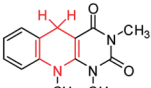
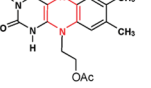
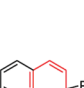
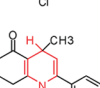
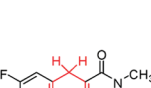
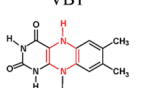
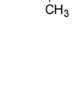
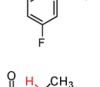
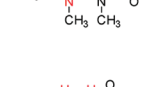
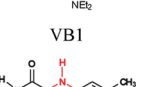
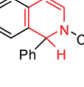
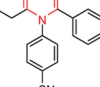
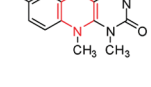
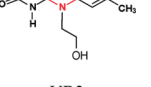
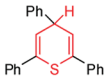
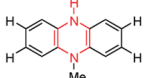
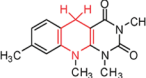
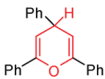
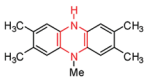
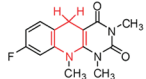
Compd.	ΔH_{H}	Compd.	ΔH_{H}	Compd.	ΔH_{H}	Compd.	ΔH_{H}
	59.1		78.7		89.2		85.1
	58.9		92.9		116.6		81.8
	57.3		67.9		99.0		85.3
	65.9		74.7		107.8		78.7
	64.6		68.5		108.7		86.8
	79.6		68.9		85.2		96.4
	86.6		68.7		77.1		76.9
	70.1		66.1		79.1		84.5
	91.5		67.8		80.3		84.0
	64.4		67.0		81.0		79.0
	66.2		71.1		85.0		82.5
	87.7		69.8		82.2		82.0
	87.1		79.9		84.9		77.1

Table 4. continued

Compd.	ΔH_{H}	Compd.	ΔH_{H}	Compd.	ΔH_{H}	Compd.	ΔH_{H}
	69.6		91.1 <i>91.1^a</i>		78.8		
	69.7		83.2		80.0		

^aThe available experimental data (from ref 63) are shown in italics.

Table 5. Hydride Dissociation Energies of Six-Membered Heterocyclic Hydrides with Various Substituents (kcal/mol)

struct.	G					correlation equation
	CH ₃	H	Cl	F	CN	
1A	65.3	66.8	67.8	65.1	78.2	$\Delta H_{\text{H}}^- = 16.2\sigma_p + 66.1$ ($R = 0.938$)
2A	65.3	66.8	72.4	72.3	83.7	$\Delta H_{\text{H}}^- = 22.3\sigma_p + 68.6$ ($R = 0.973$)
1B	94.8	96.8	98.3	96.3	111.4	$\Delta H_{\text{H}}^- = 20.5\sigma_p + 96.3$ ($R = 0.957$)
2B	93.3	96.8	100.2	99.5	114.3	$\Delta H_{\text{H}}^- = 24.9\sigma_p + 96.9$ ($R = 0.983$)
1C	94.6	96.3	96.6	93.6	104.0	$\Delta H_{\text{H}}^- = 11.8\sigma_p + 95.2$ ($R = 0.912$)
2C	94.2	96.3	101.3	100.5	112.8	$\Delta H_{\text{H}}^- = 22.5\sigma_p + 97.5$ ($R = 0.984$)
1D	63.3	63.7	69.6	68.6	77.3	$\Delta H_{\text{H}}^- = 17.4\sigma_p + 69.8$ ($R = 0.970$)
2D	62.8	63.7	69.4	69.6	78.6	$\Delta H_{\text{H}}^- = 19.2\sigma_p + 65.8$ ($R = 0.961$)
1E	87.6	88.1	94.2	94.0	100.5	$\Delta H_{\text{H}}^- = 15.8\sigma_p + 90.4$ ($R = 0.943$)
2E	85.4	88.1	94.7	94.6	103.8	$\Delta H_{\text{H}}^- = 21.7\sigma_p + 89.9$ ($R = 0.961$)
1F	83.8	83.8	89.3	89.1	94.3	$\Delta H_{\text{H}}^- = 13.0\sigma_p + 86.0$ ($R = 0.931$)
2F	82.8	83.8	89.3	89.3	96.4	$\Delta H_{\text{H}}^- = 16.4\sigma_p + 85.8$ ($R = 0.955$)

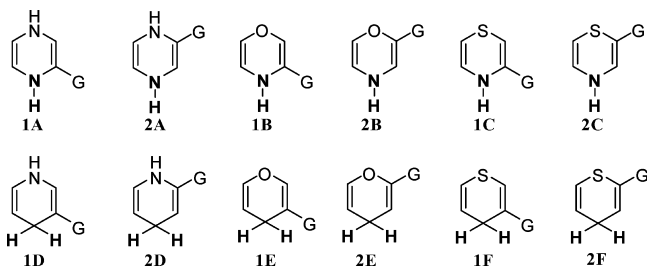


Figure 4. Structures of the selected six-membered heterocyclic hydrides (with the hydride center shown in bold).

to the heterocyclic organic hydride will further increase the hydride dissociation energies by 9.4–29.0 kcal/mol. This is somewhat unexpected since the expansion of the π system will help the delocalization of the positive charges formed after hydride dissociation, which may lead to a smaller hydride dissociation energies. However, besides the delocalization of the positive charges, the expansion of the π system will also dramatically influence the aromaticity of the cation formed after hydride dissociation. Therefore, it will be intriguing to study the aromaticity of the cations formed after hydride dissociation.

For the evaluation of aromaticity, several indices are used.^{133–138} The first index being evaluated is the HOMO–LUMO energy

gap.¹³⁹ The HOMO and LUMO energies are calculated at the B3LYP/6-311++G(2df,2p) level of theory using the structures obtained at the B3LYP/6-31G(2df,p) level of theory. Although the DFT Kohn–Sham orbitals are just “pseudo” orbitals and do not obey Koopmans’ theorem,¹⁴⁰ previous studies have shown that the HOMO–LUMO gap obtained by density functional theory can still be in good accordance with the experiments.¹⁴¹ The second index being evaluated is Bird’s index, I , which is based on the bond length/order alternation to measure the magnitude of aromaticity.¹³⁸ It is calculated using the following equations:¹⁴²

$$I = 100(1 - V/V_K), V$$

$$= 100\sqrt{N} / \sum (N - \bar{N})^2 / n, N$$

$$= a/R^2 - b$$

V_K is the value of V for the corresponding nondelocalized Kekule form with alternating single and double bonds. N is readily calculated from the individual bond lengths R in the aromatic system, where a and b are constants.¹³⁷ \bar{N} is the arithmetic mean of N . The individual bond lengths R are readily obtained from the structures optimized at the B3LYP/6-31G-(2df, p) level of theory. The last index we used to evaluate the aromaticity is HOMA (Harmonic Oscillator Measure of Aromaticity) index.^{141–147} Like Bird’s index, HOMA is also based on the bond lengths of the molecules. It is calculated by the equation below, where $R(\text{CC})_{\text{opt}}$, $R(\text{CX})_{\text{opt}}$, $R(\text{CY})_{\text{opt}}$, and $R(\text{XY})_{\text{opt}}$ refer to the optimal bond lengths for carbon–carbon, carbon–X, carbon–Y, and X–Y bonds involved in the aromatic system. R_i is the actual bond length in the aromatic system; α is the empirical constant. The values of R_{opt} and α are available in the literature.¹⁴³ The actual bond lengths are readily obtained from the structures optimized at the B3LYP/6-31G(2df,p) level of theory.

$$\text{HOMA} = 1 - \{ \alpha(\text{CC}) \sum [R(\text{CC})_{\text{opt}} - R_i]^2$$

$$+ \alpha(\text{CX}) \sum [R(\text{CX})_{\text{opt}} - R_i]^2$$

$$+ \alpha(\text{CY}) \sum [R(\text{CY})_{\text{opt}} - R_i]^2$$

$$+ \alpha(\text{XY}) \sum [R(\text{XY})_{\text{opt}} - R_i]^2 \} / n$$

As shown in Figure 6, all three indices, the HOMO–LUMO gap, Bird’s index, and HOMA, of the cations without fused benzene rings are larger than those for the corresponding cations with an expanded π system. This clearly indicates that the expansion of the π system will decrease the aromaticity of the cations and make the cations less thermodynamically stable and thus lead to an increase in the hydride dissociation energy.

Considering that solvation energies are also an important factor in determining hydride dissociation energies, we suspect

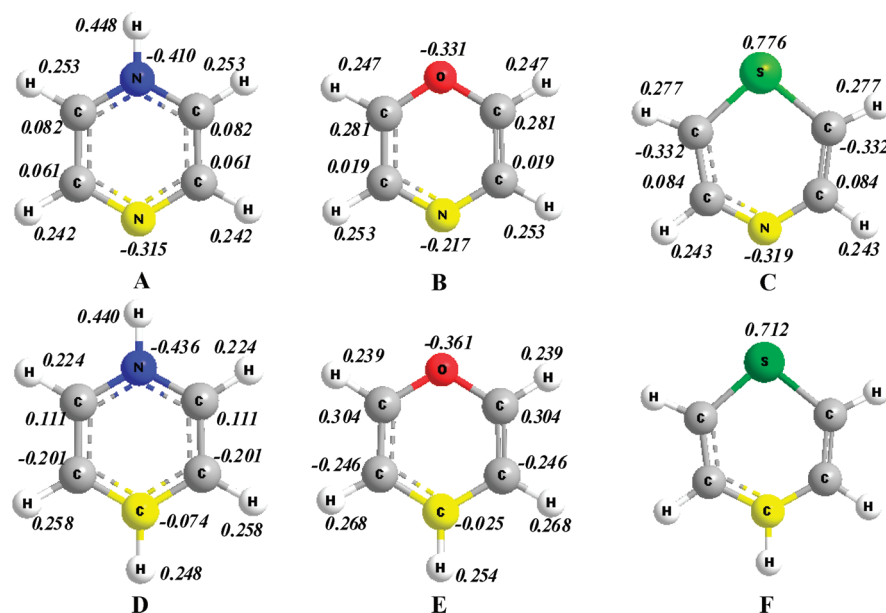


Figure 5. Natural atomic charges (in italics) of six categories of six-membered heterocyclic hydrides (hydride centers are shown in yellow; all data are calculated at the B3LYP/6-311++G(2df,2p) level of theory with structures obtained at the B3LYP/6-31G(2df,p) level of theory).

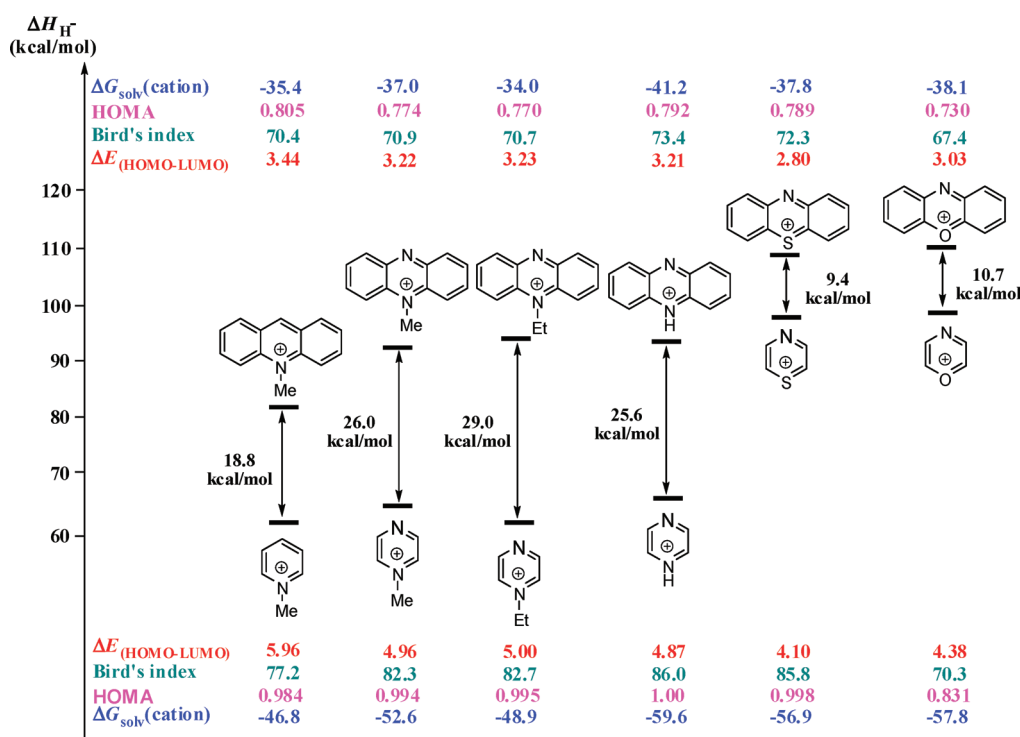


Figure 6. Hydride dissociation energies, solvation energies of cation (in kcal/mol), HOMA, Bird index, and HOMO-LUMO (in eV) energy gap of different π systems (HOMO and LUMO energies were calculated at the B3LYP/6-311++G(2df,2p) level of theory using structures obtained at the B3LYP/6-31G(2df,p) level of theory).

that the changes in solvation effect caused by the changes of the size of the π systems will also dramatically affect the hydride dissociation energy. As shown in Figure 6, it can be seen that with the fused benzene ring, the solvation energies of cations will be further decreased by at least 10 kcal/mol. The fused benzene ring may affect solvation energies in two ways: first, as the delocalization of the positive charges will be increased by the fused benzene ring, the electrostatic interaction between the solvent and the cation will be decreased; second, the

introduction of the benzene rings will increase the steric inhibition of the solvent to the cation center and thus decrease the solvation energies. In conclusion, the increase of the hydride dissociation caused by expanding the size of the π system is attributed to the decrease of both the aromaticity and the solvation energies of the cations formed after hydride dissociation.

3.4. Correlation between Different Types of Six-Membered Heterocyclic Hydrides. With the data provided in Table 5, we are curious to know whether or not there exist

Table 6. Correlation between Different Types of Six-Membered Heterocyclic Organic Hydrides

Entry	Type Y	Type X	Correlation equation	Correlation coefficient
1			$\Delta H_{\text{H}}(\text{Y}) = 1.04 \Delta H_{\text{H}}(\text{X}) + 26.8$	0.974
2			$\Delta H_{\text{H}}(\text{Y}) = 0.92 \Delta H_{\text{H}}(\text{X}) + 33.9$	0.986
3			$\Delta H_{\text{H}}(\text{Y}) = 1.03 \Delta H_{\text{H}}(\text{X}) + 22.1$	0.989
4			$\Delta H_{\text{H}}(\text{Y}) = 0.82 \Delta H_{\text{H}}(\text{X}) + 32.0$	0.993
5			$\Delta H_{\text{H}}(\text{Y}) = 0.73 \Delta H_{\text{H}}(\text{X}) + 17.4$	0.901

correlations between different types of six-membered heterocyclic hydrides. This correlation, if it exists, will provide an alternative way to estimate the hydride dissociation energies of unknown species. As shown in Table 6, excellent correlation is generated between the heterocyclic hydrides with the same hydride center, and the correlation coefficients range from 0.974 to 0.993. However, the correlation between compounds with different hydride center is poor; i.e., the correlation coefficient between 1,4-dihydropyridine and 1,4-dihydropyrazine type organic hydrides is only 0.9012 (entry 5), suggesting that the same structural modifications may exert different electronic and steric effects on C–H and N–H hydride centers.

4. CONCLUSION

In the present study, we developed a new multilayer composite *ab initio* method, ONIOM-G4, and found that it can accurately estimate the hydride dissociation energies of diverse sizable organic hydrides. With this method, an extensive hydride dissociation energy scale containing over 100 six-membered heterocyclic hydrides has been established. The hydride dissociation energies of six categories of organic hydrides generally increase in the following order: 1,4-dihydropyridine < 1,4-dihydropyrazine < 4H-thiopyran < 4H-pyran < 1,4-thiazine \approx 1,4-oxazine. The *meta* and *ortho* substituent effects for these six categories of organic hydrides have been systematically studied. The results show that electron withdrawing group will increase the hydride dissociation energies while the electron donating group will decrease it. The *meta* substituent with respect to the hydride center was found to exert a stronger influence on the hydride dissociation energies than the *ortho* substituent, which was related to the difference in positive charge distribution between the *meta* and *ortho* positions. We also studied the effect of aromaticity on hydride dissociation energy and found that expanding the size of the π system will dramatically increase the hydride dissociation energy. This is attributed to the decrease of both aromaticity and solvation energies. Finally, good linear relationships were found between different types of organic hydrides with same hydride center. These results would provide further insight into understanding the hydride donating abilities of the six-membered heterocyclic hydrides and the related biological and pharmaceutical processes.

■ ASSOCIATED CONTENT

Supporting Information

Structures of heterocyclic organic hydrides, single-point energies, zero-point vibrational energies, and solvation energies.

This information is available free of charge via the Internet at <http://pubs.acs.org>.

■ AUTHOR INFORMATION

Corresponding Author

*E-mail: shijing@ustc.edu.cn.

■ ACKNOWLEDGMENTS

This study was supported by the National Natural Science Foundation of China (No. 20832004, 20902088), the special grade of the financial support from China Postdoctoral Science Foundation (No. 201003321), and the Fundamental Research Funds for the Central Universities (Grant No. WK2060190008). We also thank the USTC-HP and Shanghai Supercomputer Center for the computational resources.

■ REFERENCES

- (1) Bruce, T. C. Mechanisms of flavin catalysis. *Acc. Chem. Res.* **1980**, *13*, 256–262.
- (2) Walsh, C. Flavin coenzymes: at the crossroads of biological redox chemistry. *Acc. Chem. Res.* **1980**, *13*, 148–155.
- (3) Walsh, C. Naturally occurring 5-deazaflavin coenzymes: biological redox roles. *Acc. Chem. Res.* **1986**, *19*, 216–221.
- (4) Fitzpatrick, P. F. Substrate Dehydrogenation by Flavoproteins. *Acc. Chem. Res.* **2001**, *34*, 299–307.
- (5) Murakami, Y.; Kikuchi, J.-L.; Hiseada, Y.; Hayashida, O. Artificial Enzymes. *Chem. Rev.* **1996**, *96*, 721–758.
- (6) Stout, D. M.; Meyers, A. I. Recent advances in the chemistry of dihydropyridines. *Chem. Rev.* **1982**, *82*, 223–243.
- (7) Eisner, U.; Kuthan, J. Chemistry of dihydropyridines. *Chem. Rev.* **1972**, *72*, 1–42.
- (8) Finer-Moore, J. S.; Santi, D. V.; Stroud, R. M. Lessons and Conclusions from Dissecting the Mechanism of a Bisubstrate Enzyme: Thymidylate Synthase Mutagenesis, Function, and Structure. *Biochemistry* **2003**, *42*, 248–256.
- (9) Hong, B. Y.; Haddad, M.; Maley, F.; Jensen, J. H.; Kohen, A. Hydride Transfer versus Hydrogen Radical Transfer in Thymidylate Synthase. *J. Am. Chem. Soc.* **2006**, *128*, 5636–5637.
- (10) Neta, P. Reactions of hydrogen atoms in aqueous solutions. *Chem. Rev.* **1972**, *72*, 533–543.
- (11) Gebicki, J.; Marcinek, A.; Zielonka, J. Transient Species in the Stepwise Interconversion of NADH and NAD. *Acc. Chem. Res.* **2004**, *37*, 379–386.
- (12) Yuasa, J.; Fukuzumi, S. Mechanistic Borderline between One-Step Hydrogen Transfer and Sequential Transfers of Electron and Proton in Reactions of NADH Analogues with Triplet Excited States of Tetrazines and Ru(bpy)₃²⁺. *J. Am. Chem. Soc.* **2006**, *128*, 14281–14292.

- (13) Ellis, W. W.; Raebiger, J. W.; Curtis, C. J.; Bruno, J. W.; DuBois, D. L. Hydricities of BzNADH , $\text{C}_5\text{H}_5\text{Mo}(\text{PMe}_3)(\text{CO})_2\text{H}$, and $\text{C}_5\text{Me}_5\text{Mo}(\text{PMe}_3)(\text{CO})_2\text{H}$ in Acetonitrile. *J. Am. Chem. Soc.* **2004**, *126*, 2738–2743.
- (14) Reichenbach-Klinke, R.; Kruppa, M.; König, B. NADH Model Systems Functionalized with $\text{Zn}(\text{II})$ -Cyclen as Flavin Binding Site-Structure Dependence of the Redox Reaction within Reversible Aggregates. *J. Am. Chem. Soc.* **2002**, *124*, 12999–13007.
- (15) Bartlett, P. N.; Simon, E. Measurement of the Kinetic Isotope Effect for the Oxidation of NADH at a Poly(aniline)-Modified Electrode. *J. Am. Chem. Soc.* **2003**, *125*, 4014–4015.
- (16) Powell, F. M.; Wu, J. C.; Bruce, T. C. Ferricyanide oxidation of dihydropyridines and analogs. *J. Am. Chem. Soc.* **1984**, *106*, 3850–3856.
- (17) Luo, J.; Bruce, T. C. Dynamic Structures of Horse Liver Alcohol Dehydrogenase (HLADH): Results of Molecular Dynamics Simulations of HLADH-NAD⁺-PhCH₂OH, HLADH-NAD⁺-PhCH₂O⁻, and HLADH-NADH-PhCHO. *J. Am. Chem. Soc.* **2001**, *123*, 11952–11959.
- (18) Andrew, T. L.; Swager, T. M. A Fluorescence Turn-On Mechanism to Detect High Explosives RDX and PETN. *J. Am. Chem. Soc.* **2007**, *129*, 7254–7255.
- (19) Miller, L. L.; Valentine, J. R. On the electron-proton-electron mechanism for 1-benzyl-1,4-dihydronicotinamide oxidations. *J. Am. Chem. Soc.* **1988**, *110*, 3982–3989.
- (20) Anne, A.; Fraoua, S.; Grass, V.; Moiroux, J.; Savéant, J.-M. The Role of Homolytic Bond Dissociation Energy in the Deprotonation of Cation Radicals. Examples in the NADH Analogues Series. *J. Am. Chem. Soc.* **1998**, *120*, 2951–2958.
- (21) Zhu, X.-Q.; Liu, Y.-C.; Wang, H.-Y.; Wang, W. A Remarkable Kinetic Isotope Effect in One-Electron Transfer from 1-Benzyl-1,4-dihydronicotinamide. *J. Org. Chem.* **1999**, *64*, 8982–8983.
- (22) Pestovsky, O.; Bakac, A.; Espenson, J. H. Kinetics and Mechanism of the Oxidation of 10-Methyl-9,10-dihydroacridine by Chromium(VI,V,IV): Electron vs Hydrogen Atom vs Hydride Transfer. *J. Am. Chem. Soc.* **1998**, *120*, 13422–13428.
- (23) Xu, H. J.; Liu, Y. C.; Fu, Y.; Wu, Y. D. Catalytic Hydrogenation of α,β -Epoxy Ketones to Form β -Hydroxy Ketones Mediated by an NADH Coenzyme Model. *Org. Lett.* **2006**, *8*, 3449–3451.
- (24) Zhang, B.-L.; Zhu, X.-Q.; Lu, J.-Y.; He, J.; Wang, P. G.; Cheng, J.-P. Polysiloxane-Supported NAD(P)H Model 1-Benzyl-1,4-dihydronicotinamide: Synthesis and Application in the Reduction of Activated Olefins. *J. Org. Chem.* **2003**, *68*, 3295–3298.
- (25) Zhu, X.-Q.; Wang, H.-Y.; Wang, J.-S.; Liu, Y.-C. Application of NAD(P)H Model Hantzsch 1,4-Dihydropyridine as a Mild Reducing Agent in Preparation of Cyclo Compounds. *J. Org. Chem.* **2001**, *66*, 344–347.
- (26) Ouellet, S. G.; Tuttle, J. B.; MacMillan, D. W. C. Enantioselective Organocatalytic Hydride Reduction. *J. Am. Chem. Soc.* **2005**, *127*, 32–33.
- (27) Hoffmann, S.; Seayad, A. M.; List, B. A Powerful Brønsted Acid Catalyst for the Organocatalytic Asymmetric Transfer Hydrogenation of Imines. *Angew. Chem., Int. Ed.* **2005**, *44*, 7424–7427.
- (28) Storer, R. I.; Carrera, D. E.; Ni, Y.; MacMillan, D. W. C. Enantioselective Organocatalytic Reductive Amination. *J. Am. Chem. Soc.* **2006**, *128*, 84–86.
- (29) Rueping, M.; Sugiono, E.; Azap, T. C.; Theissmann, M. B. Enantioselective Brønsted Acid Catalyzed Transfer Hydrogenation: Organocatalytic Reduction of Imines. *Org. Lett.* **2005**, *7*, 3781–3783.
- (30) Rueping, M.; Antonchick, A. P.; Theissmann, T. A Highly Enantioselective Brønsted Acid Catalyzed Cascade Reaction: Organocatalytic Transfer Hydrogenation of Quinolines and their Application in the Synthesis of Alkaloids. *Angew. Chem., Int. Ed.* **2006**, *45*, 3683–3686.
- (31) Heller, A. Electrical wiring of redox enzymes. *Acc. Chem. Res.* **1990**, *23*, 128–134.
- (32) Garza, L.; Jeong, G.; Liddell, P. A.; Sotomura, T.; Moore, T. A.; Moore, A. L.; Gust, D. Enzyme-Based Photoelectrochemical Biofuel Cell. *J. Phys. Chem. B* **2003**, *107*, 10252–10260.
- (33) Dueymes, C.; Decout, J. L.; Peltie, P.; Fontecave, M. Fluorescent Deazaflavin–Oligonucleotide Probes for Selective Detection of DNA. *Angew. Chem., Int. Ed.* **2002**, *41*, 486–489.
- (34) Yan, P.; Holman, M. W.; Robustelli, P.; Chowdhury, A.; Ishak, F. I.; Adams, D. M. Molecular Switch Based on a Biologically Important Redox Reaction. *J. Phys. Chem. B* **2005**, *109*, 130–137.
- (35) Strohbach, D.; Novak, N.; Müller, S. Redox-Active Riboswitching: Allosteric Regulation of Ribozyme Activity by Ligand-Shape Control. *Angew. Chem., Int. Ed.* **2006**, *45*, 2127–2129.
- (36) Trieflinger, C.; Rurack, K.; Daub, J. Turn ON/OFF your LOV light[†]: Borondipyrromethene–Flavin Dyads as Biomimetic Switches Derived from the LOV Domain. *Angew. Chem., Int. Ed.* **2005**, *44*, 2288–2291.
- (37) Schwarz, D. E.; Cameron, T. M.; Hay, P. J.; Scott, B. L.; Tumas, W.; Thorn, D. L. Hydrogen evolution from organic “hydrides”. *Chem. Commun.* **2005**, *47*, 5919–5921.
- (38) Zhang, D.; Wu, L. Z.; Zhou, L.; Yang, Q. Z.; Zhang, L. P.; Tung, C. H. Photocatalytic Hydrogen Production from Hantzsch 1,4-Dihydropyridines by Platinum(II) Terpyridyl Complexes in Homogeneous Solution. *J. Am. Chem. Soc.* **2004**, *126*, 3440–3441.
- (39) Zhu, X.-Q.; Cao, L.; Liu, Y.; Yang, Y.; Lu, J.-Y.; Wang, J.-S.; Cheng, J.-P. Thermodynamics and Kinetics of the Hydride-Transfer Cycles for 1-Aryl-1,4-dihydronicotinamide and Its 1,2-Dihydroisomer. *Chem.—Eur. J.* **2003**, *9*, 3937–3945.
- (40) Gelbard, G.; Lin, J.; Roques, N. Reductions with NADH models. 3. The high reactivity of Hantzsch amides. *J. Org. Chem.* **1992**, *57*, 1789–1793.
- (41) Kanomata, N.; Suzuki, M.; Yoshida, M.; Nakata, T. Biomimetic Oxidation of Aldehyde with NAD⁺ Models: Glycolysis-Type Hydrogen Transfer in an NAD⁺/NADH Model System. *Angew. Chem., Int. Ed.* **1998**, *37*, 1410–1412.
- (42) Mikata, Y.; Hayashi, K.; Mizukami, K.; Matsumoto, S.; Yano, S.; Yamazaki, N.; Ohno, A. Highly reactive and stereospecific reaction of quinoline-type NADH model compounds with methyl benzoylformate. *Tetrahedron Lett.* **2000**, *41*, 1035–1038.
- (43) Deno, N. C.; Peterson, J.; Saines, G. S. The hydride-transfer reaction. *Chem. Rev.* **1960**, *60*, 7–14.
- (44) Berg, J. M.; Tymoczko, J. L.; Stryer, L. *Biochemistry*, 6th ed.; W. H. Freeman: San Francisco, CA, 2008; p 510.
- (45) Schomburg, D.; Schomburg, I.; Chang, A.; Stephan, D. *Enzyme Handbook*; Springer: New York, 2005; pp 43–67.
- (46) Kuthan, J.; Kurfurst, A. Development in dihydropyridine chemistry. *Ind. Eng. Chem. Prod. Res. Dev.* **1982**, *21*, 191–261.
- (47) Birkmayer, G. NADH: The Energizing Coenzyme; NTC/contemporary: Lincolnwood, IL, 1998.
- (48) Van, Q. L.; Schwarzkopf, B.; Bacher, A.; Keller, P. J.; Lee, S.; Floss, H. G. Biosynthesis of 7,8-didemethyl-8-hydroxy-5-deazariboflavin, the chromophoric moiety of coenzyme F420. *J. Am. Chem. Soc.* **1985**, *107*, 8300–8301.
- (49) Stroud, R. M.; Finer-Moore, J. S. Conformational Dynamics along an Enzymatic Reaction Pathway: Thymidylate Synthase, “the Movie”. *Biochemistry* **2003**, *42*, 239–247.
- (50) Karrer, P. The Chemistry of Vitamins A and C. *Chem. Rev.* **1934**, *14*, 17–30.
- (51) Handoo, K. L.; Cheng, J.-P.; Parker, V. D. Hydride affinities of organic radicals in solution. A comparison of free radicals and carbenium ions as hydride ion acceptors. *J. Am. Chem. Soc.* **1993**, *115*, 5067–5072.
- (52) Zhu, X.-Q.; Li, H.-R.; Li, Q.; Ai, T.; Lu, J.-Y.; Yang, Y.; Cheng, J.-P. Determination of the C4-H bond dissociation energies of NADH models and their radical cations in acetonitrile. *Chem.—Eur. J.* **2003**, *9*, 871–880.
- (53) Chikashita, H.; Ide, H.; Itoh, K. 1,3-Dimethyl-2-phenylbenzimidazole as a novel and efficient reagent for mild reductive dehalogenation of α -halo carbonyl compounds and acid chlorides. *J. Org. Chem.* **1986**, *51*, 5400–5405.
- (54) Lee, I.-S. H.; Jeoung, E. H.; Kreevoy, M. M. Marcus theory of a parallel effect on α for hydride transfer reaction between NAD(+) analogues. *J. Am. Chem. Soc.* **1997**, *119*, 2722–2728.

- (55) Lee, I.-S. H.; Jeoung, E. H. Reactivities of five-membered heterocycles in hydride transfer reactions. *J. Org. Chem.* **1998**, *63*, 7275–7279.
- (56) Hapiot, P.; Moiroux, J.; Savéant, J.-M. Electrochemistry of NADH/NAD⁺ analogs. A detailed mechanistic kinetic and thermodynamic analysis of the 10-methylacridan/10-methylacridinium couple in acetonitrile. *J. Am. Chem. Soc.* **1990**, *112*, 1337–1343.
- (57) Anne, A.; Moiroux, J. Redox potentials and acid-base equilibria of NADH/NAD⁺ analogs in acetonitrile. *J. Org. Chem.* **1990**, *55*, 4608–4614.
- (58) Klippenstein, J.; Arya, P. D.; Wayner, D. M. Relative bond dissociation energies for some NADH model compounds from hydride transfer/electron transfer equilibria in acetonitrile. *J. Org. Chem.* **1991**, *56*, 6736–6737.
- (59) Zhu, X.-Q.; Tan, Y.; Cao, C.-T. Thermodynamic Diagnosis of the Properties and Mechanism of Dihydropyridine-Type Compounds as Hydride Source in Acetonitrile with “Molecule ID Card”. *J. Phys. Chem. B* **2010**, *114*, 2058–2075.
- (60) Zhu, X.-Q.; Zhang, M.-T.; Yu, A.; Wang, C.-H.; Cheng, J.-P. Hydride, hydrogen atom, proton, and electron transfer driving forces of various five-membered heterocyclic organic hydrides and their reaction intermediates in acetonitrile. *J. Am. Chem. Soc.* **2008**, *130*, 2501–2516.
- (61) Zhu, X.-Q.; Zhang, M.; Liu, Q.-Y.; Wang, X.-X.; Zhang, J.-Y.; Cheng, J.-P. A facile experimental method to determine the hydride affinity of polarized olefins in acetonitrile. *Angew. Chem., Int. Ed.* **2006**, *45*, 3954–3957.
- (62) Zhu, X.-Q.; Liang, H.; Cheng, J.-P. Hydride Affinities of Cumulated, Isolated, and Conjugated Dienes in Acetonitrile. *J. Org. Chem.* **2008**, *73*, 8403–8410.
- (63) Zhu, X.-Q.; Dai, Z.; Yu, A.; Wu, S.-A.; Cheng, J.-P. Driving forces for the mutual conversions between phenothiazines and their various reaction intermediates in acetonitrile. *J. Phys. Chem. B* **2008**, *112*, 11694–11707.
- (64) Zhu, X.-Q.; Liu, Q.-Y.; Chen, Q.; Mei, L.-R. Hydride, Hydrogen, Proton, and Electron Affinities of Imines and Their Reaction Intermediates in Acetonitrile and Construction of Thermodynamic Characteristic Graphs (TCGs) of Imines as a “Molecule ID Card”. *J. Org. Chem.* **2010**, *75*, 789–808.
- (65) Waksman, S. A.; Woodruff, H. B. Bacteriostatic and bactericidal substances produced by a soil actinomycetes. *Proc. Soc. Exper. Biol.* **1940**, *45*, 609–614.
- (66) Sobell, H. Actinomycin and DNA transcription. *Proc. Natl. Acad. Sci.* **1985**, *82*, 5328–5331.
- (67) Nakajima, J.; Tanaka, Y.; Yamazaki, M.; Saito, K. Reaction mechanism from leucoanthocyanidin to anthocyanidin 3-glucoside, a key reaction for coloring in anthocyanin biosynthesis. *J. Biol. Chem.* **2001**, *276*, 25797–25803.
- (68) Kong, J. M.; Chia, L. S.; Goh, N. K.; Chia, T. F.; Brouillard, R. Analysis and biological activities of anthocyanins. *Phytochemistry* **2003**, *64*, 923–933.
- (69) Winkel-Shirley, B. Flavonoid biosynthesis. A colorful model for genetics, biochemistry, cell biology, and biotechnology. *Plant Physiol.* **2001**, *126*, 485–493.
- (70) Holton, T. A.; Cornish, E. C. Genetics and Biochemistry of Anthocyanin Biosynthesis. *Plant Cell* **1995**, *7*, 1071–1083.
- (71) Lee, C.; Yang, W.; Parr, R. G. Development of the Colle-Salvetti correlation-energy formula into a functional of the electron density. *Phys. Rev. B* **1988**, *37*, 785–789.
- (72) Miehlich, B.; Savin, A.; Stoll, H.; Preuss, H. Results obtained with the correlation energy density functionals of Becke and Lee, Yang and Parr. *Chem. Phys. Lett.* **1989**, *157*, 200–206.
- (73) Zhu, X.-Q.; Wang, C.-H.; Liang, H.; Cheng, J.-P. Theoretical prediction of the hydride affinities of various p- and o-quinones in DMSO. *J. Org. Chem.* **2007**, *72*, 945–956.
- (74) Feng, Y.; Liu, L.; Wang, J. T.; Huang, H.; Guo, Q. X. Assessment of experimental bond dissociation energies using composite ab initio methods and evaluation of the performances of density functional methods in the calculation of bond dissociation energies. *J. Chem. Inf. Comput. Sci.* **2003**, *43*, 2005–2013.
- (75) Check, C. E.; Gilbert, T. M. Progressive systematic underestimation of reaction energies by the B3LYP model as the number of C-C bonds increases: Why organic chemists should use multiple DFT models for calculations involving polycarbon hydrocarbons. *J. Org. Chem.* **2005**, *70*, 9828–9834.
- (76) Wodrich, M. D.; Corminboeuf, C.; Schleyer, P. v. R. Systematic errors in computed alkane energies using B3LYP and other popular DFT functionals. *Org. Lett.* **2006**, *8*, 3631–3634.
- (77) Zheng, W.-R.; Fu, Y.; Guo, Q.-X. G3//BMK and its application to calculation of bond dissociation enthalpies. *J. Chem. Theory Comput.* **2008**, *4*, 1324–1331.
- (78) Pople, J. A.; Head-Gordon, M.; Fox, D. J.; Raghavachari, K.; Curtiss, L. A. Gaussian-1 theory: A general procedure for prediction of molecular energies. *J. Chem. Phys.* **1989**, *90*, 5622–5629.
- (79) Curtiss, L. A.; Raghavachari, K.; Trucks, G. W.; Pople, J. A. Gaussian-2 theory for molecular energies of first- and second-row compounds. *J. Chem. Phys.* **1991**, *94*, 7221–7230.
- (80) Curtiss, L. A.; Raghavachari, K.; Redfern, P. C.; Rassolov, V.; Pople, J. A. Gaussian-3 (G3) theory for molecules containing first and second-row atoms. *J. Chem. Phys.* **1998**, *109*, 7764–7776.
- (81) Curtiss, L. A.; Redfern, P. C.; Raghavachari, K. Gaussian-4 theory. *J. Chem. Phys.* **2007**, *126*, 084108.
- (82) Chan, B.; Deng, J.; Radom, L. G4(MP2)-6X: A Cost-Effective Improvement to G4(MP2). *J. Chem. Theory Comput.* **2011**, *7*, 112–120.
- (83) Martin, J. M. L.; de Oliveira, G. Towards standard methods for benchmark quality ab initio thermochemistry - W1 and W2 theory. *J. Chem. Phys.* **1999**, *111*, 1843–1856.
- (84) Boese, A. D.; Oren, M.; Atasoylu, O.; Martin, J. M.; Kállay, M.; Gauss, J. W3 theory: Robust computational thermochemistry in the kJ/mol accuracy range. *J. Chem. Phys.* **2004**, *120*, 4129–4141.
- (85) Karton, A.; Rabinovich, E.; Martin, J. M. L.; Ruscic, B. W4 theory for computational thermochemistry: In pursuit of confident sub-kJ/mol predictions. *J. Chem. Phys.* **2006**, *125*, 144108.
- (86) Ochterski, J. W.; Petersson, G. A.; Montgomery, J. A. Jr. A complete basis set model chemistry. 5. Extensions to six or more heavy atoms. *J. Chem. Phys.* **1996**, *104*, 2598–2619.
- (87) Montgomery, J. A. Jr.; Frisch, M. J.; Ochterski, J. W.; Petersson, G. A. A complete basis set model chemistry. VI. Use of density functional geometries and frequencies. *J. Chem. Phys.* **1999**, *110*, 2822–2827.
- (88) Wood, G. P. F.; Radom, L.; Petersson, G. A.; Barnes, E. C.; Frisch, M. J.; Montgomery, J. A. Jr. A restricted-open-shell complete-basis-set model chemistry. *J. Chem. Phys.* **2006**, *125*, 094106.
- (89) Bond, D. Computational methods in organic thermochemistry. 1. Hydrocarbon enthalpies and free energies of formation. *J. Org. Chem.* **2007**, *72*, 5555–5566.
- (90) Qi, X.-J.; Feng, Y.; Liu, L.; Guo, Q.-X. Assessment of performance of G3B3 and CBS-QB3 methods in calculation of bond dissociation energies. *Chin. J. Chem.* **2005**, *23*, 194–199.
- (91) Danikiewicz, W. How reliable are gas-phase proton affinity values of small carbanions? A comparison of experimental data with values calculated using Gaussian-3 and CBS compound methods. *Int. J. Mass Spectrom.* **2009**, *285*, 86–94.
- (92) Garcia, Y.; Schoenebeck, F.; Legault, C. Y.; Merlic, C. A.; Houk, K. N. Theoretical Bond Dissociation Energies of Halo-Heterocycles: Trends and Relationships to Regioselectivity in Palladium-Catalyzed Cross-Coupling Reactions. *J. Am. Chem. Soc.* **2009**, *131*, 6632–6639.
- (93) Li, M.-J.; Liu, L.; Fu, Y.; Guo, Q.-X. Development of an ONIOM-G3B3 method to accurately predict C-H and N-H bond dissociation enthalpies of ribonucleosides and deoxyribonucleosides. *J. Phys. Chem. B* **2005**, *109*, 13818–13826.
- (94) Chong, S.-S.; Fu, Y.; Liu, L.; Guo, Q.-X. O-H bond dissociation enthalpies of oximes: A theoretical assessment and experimental implications. *J. Phys. Chem. A* **2007**, *111*, 13112–13125.

- (95) Fu, Y.; Wang, H.-J.; Chong, S.-S.; Guo, Q.-X.; Liu, L. An Extensive Ylide Thermodynamic Stability Scale Predicted by First-Principle Calculations. *J. Org. Chem.* **2009**, *74*, 810–819.
- (96) Cramer, C. J.; Truhlar, D. G. Continuum Solvation Models: Classical and Quantum Mechanical Implementations. *Rev. Comput. Chem.* **1995**, *6*, 1–72.
- (97) Cramer, C. J.; Truhlar, D. G. Implicit Solvation Models: Equilibria, Structure, Spectra, and Dynamics. *Chem. Rev.* **1999**, *99*, 2161–2200.
- (98) Tomasi, J.; Mennucci, B.; Cammi, R. Quantum Mechanical Continuum Solvation Models. *Chem. Rev.* **2005**, *105*, 2999–3093.
- (99) Frisch, M. J.; Trucks, G. W.; Schlegel, H. B.; Scuseria, G. E.; Robb, M. A.; Cheeseman, J. R.; Montgomery, J. A., Jr.; Vreven, T.; Kudin, K. N.; Burant, J. C.; Millam, J. M.; Iyengar, S. S.; Tomasi, J.; Barone, V.; Mennucci, B.; Cossi, M.; Scalmani, G.; Rega, N.; Petersson, G. A.; Nakatsuji, H.; Hada, M.; Ehara, M.; Toyota, K.; Fukuda, R.; Hasegawa, J.; Ishida, M.; Nakajima, T.; Honda, Y.; Kitao, O.; Nakai, H.; Klene, M.; Li, X.; Knox, J. E.; Hratchian, H. P.; Cross, J. B.; Adamo, C.; Jaramillo, J.; Gomperts, R.; Stratmann, R. E.; Yazyev, O.; Austin, A. J.; Cammi, R.; Pomelli, C.; Ochterski, J. W.; Ayala, P. Y.; Morokuma, K.; Voth, G. A.; Salvador, P.; Dannenberg, J. J.; Zakrzewski, V. G.; Dapprich, S.; Daniels, A. D.; Strain, M. C.; Farkas, O.; Malick, D. K.; Rabuck, A. D.; Raghavachari, K.; Foresman, J. B.; Ortiz, J. V.; Cui, Q.; Baboul, A. G.; Clifford, S.; Cioslowski, J.; Stefanov, B. B.; Liu, G.; Liashenko, A.; Piskorz, P.; Komaromi, I.; Martin, R. L.; Fox, D. J.; Keith, T.; Al-Laham, M. A.; Peng, C. Y.; Nanayakkara, A.; Challacombe, M.; Gill, P. M. W.; Johnson, B.; Chen, W.; Wong, M. W.; Gonzalez, C.; Pople, J. A. *Gaussian 03*, Revision D and B.05; Gaussian, Inc.: Wallingford, CT, 2004.
- (100) Petersson, G. A.; Bennett, A.; Tensfeldt, T. G.; Al-Laham, M. A.; Shirley, W. A.; Mantzaris, J. A complete basis set model chemistry. I. The total energies of closed shell atoms and hydrides of the first-row elements. *J. Chem. Phys.* **1988**, *89*, 2193–2218.
- (101) Pickett, H. M. The fitting and prediction of vibration-rotation spectra with spin interactions. *J. Mol. Spectrosc.* **1991**, *148*, 371–377.
- (102) Hay, P. J. Gaussian basis sets for molecular calculations. The representation of 3d orbitals in transition-metal atoms. *J. Chem. Phys.* **1977**, *66*, 4377–4384.
- (103) Raghavachari, K.; Binkley, J. S.; Seeger, R.; Pople, J. A. Self-consistent molecular orbital methods. XX. A basis set for correlated wave functions. *J. Chem. Phys.* **1980**, *72*, 650–654.
- (104) McLean, A. D.; Chandler, G. S. Contracted Gaussian basis sets for molecular calculations. I. Second row atoms, Z=11–18. *J. Chem. Phys.* **1980**, *72*, 5639–5648.
- (105) Raghavachari, K.; Trucks, G. W. Highly correlated systems. Excitation energies of first row transition metals Sc–Cu. *J. Chem. Phys.* **1989**, *91*, 1062–1065.
- (106) Binning, R. C. Jr.; Curtiss, L. A. Compact contracted basis-sets for 3rd-row atoms - ga-kr. *J. Comput. Chem.* **1990**, *11*, 1206–1216.
- (107) McGrath, M. P.; Radom, L. Extension of Gaussian-1 (G1) theory to bromine-containing molecules. *J. Chem. Phys.* **1991**, *94*, 511–516.
- (108) Curtiss, L. A.; McGrath, M. P.; Blaudeau, J. P.; Davis, N. E.; Binning, R. C. Jr.; Radom, L. Extension of Gaussian-2 theory to molecules containing third-row atoms Ga–Kr. *J. Chem. Phys.* **1995**, *103*, 6104–6013.
- (109) Blaudeau, J. P.; McGrath, M. P.; Curtiss, L. A.; Radom, L. Extension of Gaussian-2 (G2) theory to molecules containing third-row atoms K and Ca. *J. Chem. Phys.* **1997**, *107*, 5016–5021.
- (110) Miertus, S.; Scrocco, E.; Tomasi, J. Electrostatic interaction of a solute with a continuum - a direct utilization of abinitio molecular potentials for the prevision of solvent effects. *Chem. Phys.* **1981**, *55*, 117–129.
- (111) Miertus, S.; Tomasi, J. Approximate evaluations of the electrostatic free-energy and internal energy changes in solution processes. *Chem. Phys.* **1982**, *65*, 239–241.
- (112) Cossi, M.; Barone, V.; Cammi, J. Ab initio study of solvated molecules: A new implementation of the polarizable continuum model. *Chem. Phys. Lett.* **1996**, *255*, 327–335.
- (113) Cancès, M. T.; Mennucci, B.; Tomasi, J. A new integral equation formalism for the polarizable continuum model: Theoretical background and applications to isotropic and anisotropic dielectrics. *J. Chem. Phys.* **1997**, *107*, 3032–3037.
- (114) Mennucci, B.; Tomasi, J. Continuum solvation models: A new approach to the problem of solute's charge distribution and cavity boundaries. *J. Chem. Phys.* **1997**, *106*, 5151–5158.
- (115) Qi, X. J.; Liu, L.; Fu, Y.; Guo, Q. X. Ab initio calculations of pk(a) values of transition-metal hydrides in acetonitrile. *Organometallics* **2006**, *25*, 5879–5886.
- (116) Fu, Y.; Liu, L.; Yu, H. Z.; Wang, Y. M.; Guo, Q. X. Quantum-Chemical Predictions of Absolute Standard Redox Potentials of Diverse Organic Molecules and Free Radicals in Acetonitrile. *J. Am. Chem. Soc.* **2005**, *127*, 7227–7234.
- (117) Head-Gordon, M.; Pople, J. A.; Frisch, M. J. Mp2 energy evaluation by direct methods. *Chem. Phys. Lett.* **1988**, *153*, 503–506.
- (118) Saebo, S.; Almlöf, J. Avoiding the integral storage bottleneck in lcao calculations of electron correlation. *Chem. Phys. Lett.* **1989**, *154*, 83–89.
- (119) Frisch, M. J.; Head-Gordon, M.; Pople, J. A. A direct mp2 gradient-method. *Chem. Phys. Lett.* **1990**, *166*, 275–280.
- (120) Frisch, M. J.; Head-Gordon, M.; Pople, J. A. Semidirect algorithms for the mp2 energy and gradient. *Chem. Phys. Lett.* **1990**, *166*, 281–289.
- (121) Head-Gordon, M.; Head-Gordon, T. Analytic mp2 frequencies without 5th-order storage - theory and application to bifurcated hydrogen-bonds in the water hexamer. *Chem. Phys. Lett.* **1994**, *220*, 122–128.
- (122) Xu, X.; Goddard, W. A. III. The X3LYP extended density functional for accurate descriptions of nonbond interactions, spin states, and thermochemical properties. *Proc. Natl. Acad. Sci. U.S.A.* **2004**, *101*, 2673–2677.
- (123) Perdew, J. P. In *Electronic Structure of Solids '91*; Ziesche, P., Eschrig, H., Eds.; Akademie Verlag: Berlin, 1991.
- (124) Perdew, J. P. Density-functional approximation for the correlation-energy of the inhomogeneous electron-gas. *Phys. Rev. B* **1986**, *33*, 8822–8824.
- (125) Xu, X.; Zhang, Q.-S.; Muller, R.-P.; Goddard, W. A. An extended hybrid density functional (X3LYP) with improved descriptions of nonbond interactions and thermodynamic properties of molecular systems. *J. Chem. Phys.* **2005**, *122*, 014105.
- (126) Dapprich, S.; Komaromi, I.; Byun, K. S.; Morokuma, K.; Frisch, M. J. A new ONIOM implementation in Gaussian98. Part I. The calculation of energies, gradients, vibrational frequencies and electric field derivatives. *THEOCHEM* **1999**, *461*, 1–21.
- (127) Zenno, S.; Saigo, K. Identification of the genes encoding nad(p)h-flavin oxidoreductases that are similar in sequence to escherichia-coli fre in 4 species of luminous bacteria - photorhabdus-luminescens, vibrio-fischeri, vibrio-harveyi, and vibrio-orientalis. *J. Bacteriol.* **1994**, *176*, 3544–3551.
- (128) Iyanagi, T.; Yamazaki, I. One-electron-transfer reactions in biochemical systems 0.5. difference in mechanism of quinone reduction by nadh dehydrogenase and nad(p)h dehydrogenase (dt-diaphorase). *Biochim. Biophys. Acta* **1970**, *216*, 282–294.
- (129) Möller, I. M.; Lin, W. Membrane-bound NAD(P)H dehydrogenases in higher plant cells. *Annu. Rev. Plant Physiol.* **1986**, *37*, 309–334.
- (130) Hansch, C.; Leo, A.; Taft, R. W. A survey of Hammett substituent constants and resonance and field parameters. *Chem. Rev.* **1991**, *97*, 165–195.
- (131) Liu, L.; Fu, Y.; Liu, R.; Li, R.-Q.; Guo, Q.-X. Hammett equation and generalized Pauling's electronegativity equation. *J. Chem. Inf. Comput. Sci.* **2004**, *44*, 652–657.
- (132) Reed, A. E.; Curtiss, L. A.; Weinhold, F. Intermolecular interactions from a natural bond orbital, donor-acceptor viewpoint. *Chem. Rev.* **1988**, *88*, 899–926.
- (133) Krygowski, T. M.; Cyranski, M. K.; Czarnocki, Z.; Häfelfinger, G.; Katritzky, A. R. Aromaticity: A theoretical concept of immense practical importance. *Tetrahedron* **2000**, *56*, 1783–1796.

- (134) Aihara, J. Why are some polycyclic aromatic hydrocarbons extremely reactive? *Phys. Chem. Chem. Phys.* **1999**, *1*, 3193–3197.
- (135) Thomas, S.; Pati, A. A Comparative Study of Aromaticity in Substituted Tetracyclic and Hexacyclic Thiophenes. *J. Phys. Chem. A* **2010**, *114*, 5940–5946.
- (136) King, R. B. Three-dimensional aromaticity in polyhedral boranes and related molecules. *Chem. Rev.* **2001**, *101*, 1119–1152.
- (137) Bird, C. W. A new aromaticity index and its application to five-membered ring heterocycles. *Tetrahedron* **1985**, *41*, 1409–1414.
- (138) Bird, C. W. Heteroaromaticity VIII: the influence of (n)-under-bar-oxide formation on heterocyclic aromaticity. *Tetrahedron* **1993**, *49*, 8441–8448.
- (139) Zhou, Z.; Parr, R. G. new measures of aromaticity - absolute hardness and relative hardness. *J. Am. Chem. Soc.* **1989**, *111*, 7371–7379.
- (140) Kümmel, L.; Kronik, L. Orbital-dependent density functionals: Theory and applications. *Rev. Mod. Phys.* **2008**, *80*, 3.
- (141) De Proft, F.; Geerlings, P. Conceptual and Computational DFT in the Study of Aromaticity. *Chem. Rev.* **2001**, *101*, 1451–1464.
- (142) Bird, C. W.; Heteroaromaticity, V a unified aromaticity index. *Tetrahedron* **1992**, *48*, 335–340.
- (143) Krygowski, T. M. Crystallographic studies of intermolecular and intramolecular interactions reflected in aromatic character of pi-electron systems. *J. Chem. Inf. Comput. Sci.* **1993**, *33*, 70–78.
- (144) Kruszewski, J.; Krygowski, T. M. Definition of aromaticity basing on harmonic oscillator model. *Tetrahedron Lett.* **1972**, *13*, 3839–3842.
- (145) Krygowski, T. M.; Cyrański, M. Structural Aspects of Aromaticity. *Chem. Rev.* **2001**, *101*, 1385–1419.
- (146) Parr, R. G.; Chattaraj, P. K. Principle of maximum hardness. *J. Am. Chem. Soc.* **1991**, *113*, 1854–1855.
- (147) Chattaraj, P. K.; Roy, D. RE; Elango, M.; Subramanian, V. Stability and reactivity of all-metal aromatic and antiaromatic systems in light of the principles of maximum hardness and minimum polarizability. *J. Phys. Chem. A* **2005**, *109*, 9590–9597.